Biosorption of methylene blue dye by *Ligustrum lucidum* fruits biomass: equilibrium, isotherm, kinetic and thermodynamic studies

Panagiotis Haskis[1], Pantelis Tsolis[1], Lidia Tsiantouka[1], Paraskeyi Mpeza[1], Pantelis Barouchas[2], Georgios Giannopoulos[1], Ioannis Pashalidis[3], Ioannis Anastopoulos[1,*]

[1]Department of Agriculture, University of Ioannina, UoI Kostakii Campus, 47100 Arta, Greece

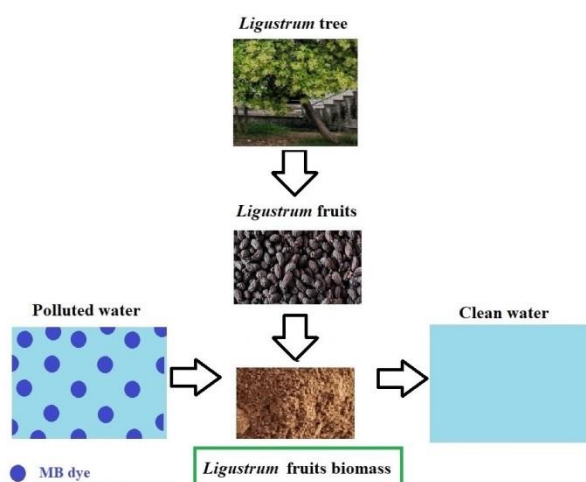[2]Department of Agriculture, University of Patras, Messolonghi Campus, 30200 Messolonghi, Greece

[3]Department of Chemistry, University of Cyprus, P.O. Box 20537, 1678 Nicosia, Cyprus

Graphical abstract

1. Introduction

Water is essential for all known life forms (do Nascimento Vieira *et al.,* 2020). Water safety has become a crucial requirement for drinking water due to increased activities that can pollute water supplies (Hosny *et al.,* 2023). Every year, a large amount of wastewater is generated and discharged untreated directly into aquatic receivers. Dyeing wastewater is one type of wastewater that requires special consideration (Zhou *et al.,* 2019). Dyes are colored compounds widely used in textiles, printing, rubber, cosmetics, plastics, and leather industries to color their products resulting in the production of vast amounts of colored wastewater (Kandisa *et al.,* 2016). To satisfy the modern needs, it is assessed that 0.7–1.6 million tons of dyes are delivered yearly, and 10–15% of this volume is disposed of as wastewater, making them a significant water pollutant (Aragaw and Bogale, 2021). Dyeing wastewater is highly toxic and potentially carcinogenic to aquatic life and human beings (Hossen *et al.,* 2022). Hence, it is essential to effectively remove the dyes from produced wastewater before releasing them into the environment (Wang *et al.,* 2022). Several techniques can be applied to clean the polluted wastewater from dyes, such as chemical precipitation, ultrafiltration, aerobic and anaerobic microbial degradation, coagulation/flocculation, advanced oxidation processes, electrochemical treatments, reverse osmosis, and adsorption (Bulgariu *et al.,* 2019). Adsorption is regarded as one of the most significant and beneficial decontamination processes (Dotto *et al.,* 2015, Dos Reis *et al.,* 2020, Pang *et al.,* 2020, Ighalo *et al.,* 2021, Santos *et al.,* 2023) because it is a fast, inexpensive, simple, sludge-free process, having high efficiency and/or selectivity, mechanical stability, and recycling facilities (Dutta *et al.,* 2021). It has been proven that using biosorbents to remove toxic dyes from wastewater is a practical, and environmentally friendly approach.

Abstract

In this work, biomass from *Ligustrum lucidum* fruits (LF) was used for the first time as a novel adsorbent to remove the Methylene Blue dye (MB) from aqueous solutions. The adsorption equilibrium was attained after 60 min, and the adsorption followed the pseudo-second-order kinetic model. The rise of temperature from 295 K to 313 K resulted in a decline in the adsorption capacity, suggesting an exothermic process. The *Langmuir* isotherm model was found to fit better the experimental adsorption data than the *Freundlich* isotherm model. The maximum monolayer adsorption capacity obtained from the *Langmuir* isotherm model at pH 5.6 was evaluated to be 95.4 mg/g and 91.8 mg/g at 295 K and 313 K, respectively. The thermodynamic studies indicated that the adsorption was a spontaneous and exothermic process with increasing randomness at the solid/solution interface. Based on FTIR and ionic strength studies, the adsorption of MB by LF mainly occurs via electrostatic interactions and the formation of outer-sphere complexes.

Ligustrum lucidum, a member of the Oleaceae family, has been widely cultivated for various cultural and medicinal purposes and traditional medicine since ancient times. The fruit is picked when fully ripe and dried for later use. It is frequently decocted with other herbs to treat various illnesses and serves as a general tonic (Fernandez *et al.,* 2020).

This is the first time that *Ligustrum lucidum* fruit biomass (LF) is used to explore its adsorptive behavior towards Methylene Blue (MB) dye. For this purpose, batch adsorption experiments were performed to investigate various adsorption parameters (initial, concentration, solution pH, contact time, temperature, ionic strength). Isotherm, kinetic, and thermodynamic studies were also performed and discussed in detail. To identify the adsorption mechanism, the effect of the ionic strength has been investigated and *FTIR* measurements have been performed before and after MB adsorption.

2.   Materials and methods

The fruits of *Ligustrum lucidum* (FL) originate from the area of the Department of Agriculture of the University of Ioannina in the Arta Campus. After being washed with deionized water to remove dirt, they were placed in an oven at 50 °C until constant weight. Then, the dried FL were grounded and converted into powder, and the final sample was passed through a 1 mm sieve. This material fraction (<1 mm) was used for all adsorption experiments.

A cationic dye MB (chemical formula: $C_{16}H_{18}N_3SCl·3H_2O$; FW: 373.9 g/mol, λ_{max} = 663 nm) was selected as a adsorbate and used without further purification.

The MB test solutions were prepared from a 1000 mg/L stock solution, which was prepared by dissolving 1 g of MB in 1 liter of distilled water.

The amount of MB adsorbed at time *t* (Eq.1) or equilibrium state (Eq.2) was evaluated using following equations:

$$q_t = \frac{(C_i - C_t)V}{m} \tag{1}$$

$$q_e = \frac{(C_i - C_e)V}{m} \tag{2}$$

Where C_i (mg/L) represents the starting MB concentration in the aqueous phase, C_t (mg/L) and C_e (mg/L) are the MB concentrations in the liquid phase at a given time (*t),* and equilibrium, respectively, *V* (L) is the liquid phase volume and *m* (g) is the mass of FL added.

Generally, the parameter under investigation was varied, whereas the others were kept constant as indicated in Table 1.

Table 1. The experimental design of the adsorption of MB by FL adsorbent. (Read from left to right on each line for the different factors). The agitation rate of 125 rpm was constant for all the experiments

	V (mL)	pH	Adsorbent dose (g)	Initial concentration (mg / L)	Contact time (min)	T (K)
FL						
pH	50	~2.0 – ~8.0	0.1*	50	1440	295
Adsorbent dose (g)	50	5.6	0.02 – 0.5	50	1440	295
Initial concentration (mg / L)	50	5.6	0.04**	20 – 300	1440	295
Contact time (min)	50	5.6	0.04**	50	0 – 120	295
T (K)	50	5.6	0.04**	20 – 300	1440	295 and 313
Ionic strength NaCl (0 – 1 M)	50	5.6	0.04**	50	1440	295

For the effect of pH 0.1 g of adsorbent was used

**For the effect of initial concentration, contact time, temperature, and ionic strength 0.04 g of adsorbent was used for better filtration*

3.   Results and discussion

3.1. Effect of pH on MB dye uptake

The adsorbent surface charge and degree of ionization of the adsorbate molecules are governed by the solution pH, which is very important regarding the adsorption process (Fakioğlu and Kalpaklı, 2022). Figure 1 shows the effect of pH on the uptake of the MB dye by the FL adsorbent in a range of pH values from ~2.0 to ~8.0. Increasing the pH value from ~2.0 to ~4.0 has led to a sharp increase in the adsorption capacity from q_e = 4.6 mg/g to q_e = 15.7 mg/g. Up to pH 5.6, a gradual increase was observed, reaching a maximum adsorption (q_e =19.7 mg/g). For pH values > 5.6, the adsorption capacity decreased slightly, and at pH ~ 8.0 the adsorption capacity values were equal to q_e =18.5 mg/g. The basic dyes (such as the MB dye) become positively charged ions when dissolved in water (Pathania *et al.,* 2017). As the pH value increases, gradual deprotonation of adsorbent surface groups occurs, resulting in an electrostatic attraction between the negatively charged surface of the adsorbent and the positively charged MB dye (Besharati *et al.,* 2018).

Gao *et al.* 2021, studied the adsorption of MB dye from sugar beet pulp (SBP) and Fe-rich SBP-based biosorbents and found that increasing the pH value of the solution of MB dye from 2.0 to 4.0 led to a sharp increase in MB dye adsorption, followed by a gradual increase in adsorption from pH 4.0 to pH 8.0. Ncibi et al. (2007) studied the adsorption of MB dye by fibers of the marine plant *Posidonia oceanica* in a pH range between 2.0 and 9.0 and found that the minimum adsorption capacity was at pH 2.0 (4.59 mg/g), then increased at a pH value of 5.0 and

with a further increase of the pH value from 6.0 to 9.0, it remained constant (4.91 mg/g). Similarly, Han *et al.* 2007, found that an increase in the pH value of the solution of MB dye from 2.5 to 4.5 positively affected its adsorption by fallen phoenix tree's leaves, while a further increase from 4.5 to a pH value of 10.0, did not affect the adsorption capacity.
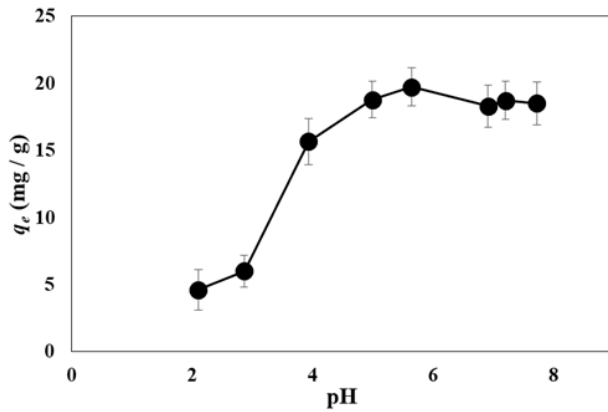

Figure 1. Effect of pH on adsorption of MB on FL. Experimental conditions: contact time 24 h, initial metal concentration 50 mg/L, adsorbent/solution ratio 0.1 g/0.05 L, agitation rate 125 rpm, temperature 295 K

3.2. Effect of adsorbent dose (FL) on MB dye uptake

Figure 2 illustrates the effect of the adsorbent dose (FL) on the biosorption of MB dye. Increasing the adsorbent dose from 0.02 g to 0.2 g led to a sharp decrease in the adsorption capacity from 63.7 mg/g to 9.1 mg/g, while with a further increase in the dose to 0.5 g, a gradual decrease in adsorption capacity (3.5 mg/g) was observed.
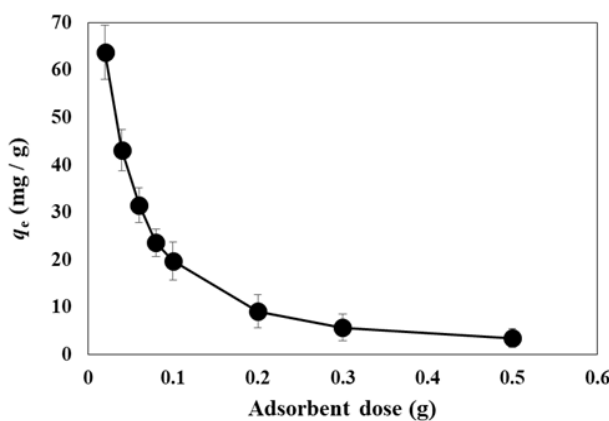

Figure 2. Effect of adsorbent dose on adsorption of MB on FL. Experimental conditions: pH 5.6, contact time 24 h, initial metal concentration 50 mg/L, volume 0.05 L, agitation rate 125 rpm, temperature 295 K

This is because the dose of adsorbent is inversely proportional to the unit adsorption capability, according to Equation (2.1). In addition, increasing the dose of the adsorbent material can lead to the formation of aggregates, leading to coverage of some active adsorption sites thus reducing the adsorption capacity (AL-Shehri *et al.*, 2022). Similar results were found by Kini et al. (2014), who studied the adsorption of MB dye by palm tree male flower biomass. More specifically, they noticed that increasing the adsorbent mass

from 0.05 to 0.3 g led to a decrease in the adsorption capacity of the adsorbent material, from 163 mg/g to 61.1 mg/g.

3.3. Effect of contact time and kinetic modeling on MB dye uptake by FL

Figure 3 shows the effect of the contact time (0 – 120 min) on the adsorption of the MB dye by the FL adsorbent. The MB adsorption was initially fast, thereafter progressively slowed down until reaching a steady state. This trend is attributed to the saturation of the existing available active sites on adsorbent with proceeding adsorption (Chen *et al.*, 2018) and to the difficulty of the remaining vacant surface sites to be occupied by MB dye molecules due to repulsive forces between the solute molecules on the solid and bulk phases (Basu *et al.*, 2018). Based on Figure 3 the adsorption of MB by FL adsorbent reached equilibrium after 60 min.

Kandisa *et al.* (2018), Alghamdi *et al.* (2021) and Amuda *et al.* (2014) studied the removal of MB dye from *Vigna Trilobata* pods, *Citrullus colocynthis* seeds, and activated carbon from *Lantana camara* stem, respectively, also concluded that ≥60 min are sufficient to achieve equilibrium.
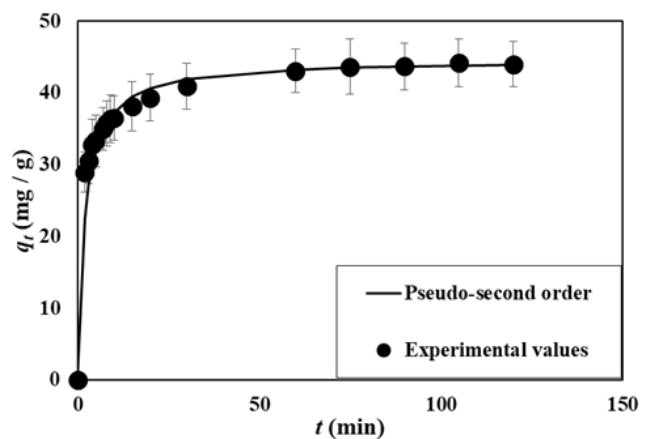

Figure 3. Effect of contact time on adsorption of MB on FL. Experimental conditions: pH 5.6, initial metal concentration 50 mg/L, adsorbent/solution ratio 0.04 g/0.05 L, agitation rate 125 rpm, temperature 295 K

Kinetic models were used to thoroughly examine the rate of the biosorption process. For that purpose, pseudo-first order (Lagergren, 1898) and pseudo-second order (Blanchard *et al.*, 1984) kinetic models were applied to the experimental kinetic data, and the estimated adsorption parameters, together with R^2 values, are shown in Table 2.

The pseudo-first-order (3) and pseudo-second-order (4) kinetic models are expressed as:

$$q_t = q_e(1\text{-}\exp^{-k_1 t}) \tag{3}$$

$$q_t = \frac{k_2 q_e^2 t}{1 + k_2 q_e t} \tag{4}$$

where q_e (mg/g) and q_t (mg/g) are the amounts of MB sorbed at equilibrium and at time *t*. K_1 (min^{-1}) and K_2 (g/mg min) are the pseudo-first and pseudo-second order equilibrium rate constants, respectively.

Table 2. Kinetic parameters obtained from pseudo-first order and pseudo-second order kinetic models for MB biosorption onto FL adsorbent. Experimental conditions: pH 5.6, initial metal concentration 50 mg/L, adsorbent/solution ratio 0.04 g/0.05 L, agitation rate 125 rpm, temperature 295 K

Pseudo-first order				Pseudo-second order		
$q_{e,exp.}$ (mg/g)	q_{e1} (mg / g)	k_1 (min^{-1})	R^2	q_{e2} (mg / g)	k_2 (g /mg min)	R^2
43.86	13.48	0.065	0.97	44.64	0.011	0.99

$q_{experimental}$: *Experimental adsorption capacity*, $q_{e1,predicted}$ *and* $q_{e2,predicted}$: *Predicted adsorption capacity from pseudo-first order and pseudo-second order kinetic models, respectively*

Based on Table 2, compared to the pseudo-first order kinetic model, the pseudo-second order kinetic model was related to higher R^2 values (0.99), and the predicted q_{e2} values were closer to the experimental $q_{e, exp}$ values. So, it can be concluded that the biosorption of MB dye by FL follows the pseudo-second-order. Similar observations were also found by Deniz and Tezel Ersanli (2022) and Nath *et al.* (2021), who studied the adsorption of MB dye by biowaste left over from the fixed oil biorefinery process of *Nigella sativa L. plant*, and okra (*Abelmoschus esculentus* L.) mucilage modified biochar, respectively. In contrast, Thabede *et al.* 2021, mentioned that the MB dye uptake by raw *Nigella sativa* L. seeds followed the pseudo-first order model.
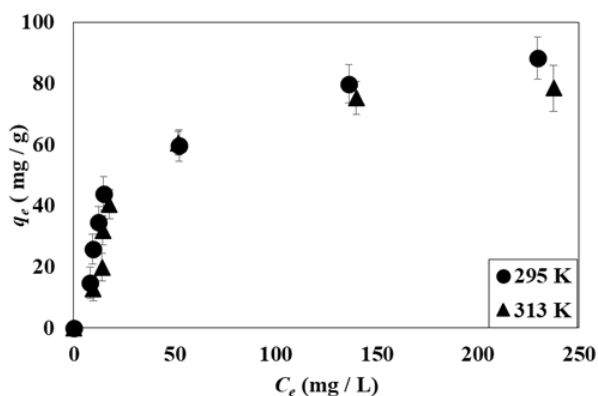

Figure 4. Adsorption isotherms of MB on FL at temperatures of 295 K and 313 K, respectively. Experimental conditions: pH 5.6, contact time 24 h, initial metal concentration 20 mg/L – 300 mg/L, adsorbent/solution ratio 0.04 g/0.05 L, agitation rate 125 rpm

Figure 4 depicts the adsorption isotherms of the MB dye by FL at two different temperatures (295 K and 313 K). Increasing the initial concentration from 20 mg/L to 300 mg/L has led to an increment in adsorption from 14.8 mg/g to 88.2 mg/g and from 12.8 mg/g to 78.3 mg/g at temperatures of 295 K and 313K, respectively. Increasing the initial concentration leads to an increase in the driving force resulting in overcoming the resistance to mass transfer of the dye from the liquid to the solid phase (Taweekarn *et al.,* 2022). Conversely, the temperature rise led to a decrease in adsorption, e.g., from 88.2 mg/g at 295 K to 78.3 mg/g at 313 K (for an initial concentration of MB dye = 300 mg/L), showing that the adsorption is an exothermic reaction (Anastopoulos and Pashalidis, 2019).

The *Langmuir* (*Langmuir*, 1918) and *Freundlich* (*Freundlich*, 1906) isotherms models were applied to the experimental data of Figure, and the corresponding parameters of the isotherm models and the coefficient of determination are shown in Table 3.

The results showed that the experimental data fit satisfactorily (R^2) to the *Langmuir* isotherm. Similar results were found by Zein *et al.* 2023 and Nipa *et al.* 2023, who studied the adsorption of MB dye by lemongrass leaves modified with citric acid and papaya bark fibers, respectively. Table 4 shows the maximum adsorption capacity for MB dye of various adsorbent materials derived from agricultural biomass/waste. The maximum adsorption capacity value of FL for MB compared to the corresponding values of various adsorbent materials listed, is considered satisfactory.

Table 3. Evaluated parameters by applying the *Langmuir* and *Freundlich* isotherm models at 295 K and 313 K, respectively. Experimental conditions: pH 5.6, contact time 24 h, initial metal concentration 20 mg/L – 300 mg/L, adsorbent/solution ratio 0.04 g/0.05 L, agitation rate 125 rpm

T (K)	Langmuir			Freundlich		
	q_{max} (mg/g)	K_L (L/mg)	R^2	K_F (mg/g) (L/mg)$^{1/n}$	n	R^2
295	95.43	0.04	0.99	9.76	2.33	0.82
313	91.80	0.03	0.99	6.76	2.05	0.79

3.4. Thermodynamic studies

Adsorption thermodynamic parameters (Gibbs free energy change (ΔG°), enthalpy change (ΔH°), and entropy change (ΔS°) are calculated at temperatures of 295 K and 313 K, according to the following thermodynamic equations (Anastopoulos and Kyzas, 2016, Lima *et al.,* 2019):

$$\Delta G^0 = -RT \ln K_e^0 \tag{5}$$

$$\Delta H^0 = R\left(\frac{T_2 \times T_1}{T_2 - T_1}\right)\ln\left(\frac{K_{e2}^0}{K_{e1}^0}\right) \tag{6}$$

$$\Delta G^0 = \Delta H^0 - T\Delta S^0 \tag{7}$$

where K_e^0 is the thermodynamic equilibrium constant (Lima *et al.,* 2019) at two studied temperatures T (K_{e1}^0 and K_{e2}^0 for 295 K and 313 K, respectively) and R (8.314 J/ mol K) is the universal gas constant.

Table 4. *The maximum adsorption capacity for MB dye of various adsorbent materials derived from agricultural biomass/waste*

Adsorbent	q_{max} (mg/g)	References
Activated carbon from rice husk	9.83	Sharma and Uma, 2010
Penicillium glabrum	16.67	Bouras *et al.,* 2021
Pristine seeds Nigella sativa L.	18.79	Thabede *et al.,* 2021
Aspergillus carbonarius	21.88	Bouras *et al.* 2021
Natural core-shell structure activated carbon beads derived from Litsea glutinosa seeds	24.68	Dao *et al.* 2021
Sawdust biochar	27.47	Nath *et al.* 2021
Carica papaya wood	32.25	Rangabhashiyam *et al.* 2018
Passiflora edulis Sims. f. flavicarpa Degener	44.70	Pavan *et al.* 2008
Paspalum maritimum	56.18	Silva *et al.* 2019
Papaya bark fiber	66.67	Nipa *et al.* 2023
Palm spathe	74.29	Djelloul *et al.* 2021
Sawdust-derived biochar modified using okra mucilage.	78.13	Nath *et al.* 2021
Terminalia catappa shell	86.22	Hevira *et al.* 2021
FL	95.43	This study

The ΔG° were found to be −23.19 kJ/mol and −23.95 kJ/mol at 295 and 313 K, respectively, suggesting that the adsorption of MB onto FL is a spontaneous process (Geng *et al.,* 2018). The ΔH^0 and the ΔS^0 were found to be −9.59 kJ/mol and 0.046 kJ/mol K, respectively. The negative value of ΔH^0 indicates that the adsorption of MB onto FL is an exothermic process (Chowdhury and Saha, 2012). The positive results of the ΔS^0 imply increasing randomness in the solid/solution system interface during adsorption. Similar results have also been found using olive tree pruning waste as an adsorbent to remove the MB dye (Fan *et al.,* 2016, Anastopoulos *et al.,* 2018).

3.5. Effect of ionic strength, FTIR spectra, and adsorption mechanism

The effect of ionic strength on the adsorption of MB by LF adsorbent was explored by changing the salt concentration using NaCl solutions of varying concentration (0 – 1 M). The results (Figure 5) showed that an increase in NaCl concentration from 0 to 1 M, decreases the amount of the adsorbed MB dye from 44 to 3.5 mg/g. Similar results have also been found by Boumediene *et al.,* 2018, who investigated the adsorption of MB by orange peel. They observed that adsorption capacity decreased from 205 to 74 mg/g when the NaCl concentration in solutions increased from 0 M to 0.1 M. This may be due to the sodium ions competing with MB dye molecules for the same adsorption sites thus reducing the adsorption intensity (Li *et al.,* 2022). Also, the thickness of the electrical double layer decreases as the ionic strength increases, resulting in a decrease in adsorption (Rani and Mahajan, 2016). The above results indicate that the adsorption process is based on electrostatic interaction between the positively charged dye molecules and the negatively charged FL surface that results in the formation of outer-sphere complexes.
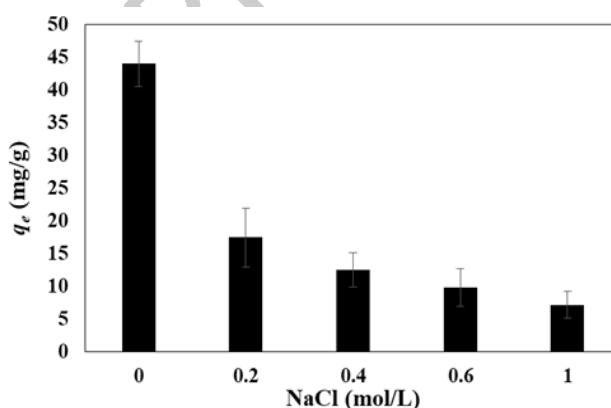

Figure 5. The effect of solution ionic strength (NaCl concentration ranged from 0 to 1 mol/L) on the adsorption of MB by FL. Experimental conditions: pH 5.6, initial concentration 50 mg/L, contact time 24 h, adsorbent/solution ratio 0.04 g/0.05 L, agitation rate 125 rpm, temperature 295 K

The predominance of electrostatic interactions and the formation of outer-sphere complexes is also indicated by the *FTIR* spectra (Figure 6), which do not show any changes in the spectrum of FL prior to and after MB adsorption. The *FTIR* spectrum of FL includes the characteristic peaks of plant-derived adsorbents such as the broad peak at 3400 cm−1 (O–H and N–H stretching vibrations), 2925 cm^{-1} (C–H vibration), 1740 cm^{-1} (C=O stretching vibration), 1625 cm^{-1} (N–H deformation vibration), and 1070 cm^{-1} (C–O stretching vibration). The additional weak peaks between 1600 cm-1 and 1000 cm-1 present in the spectrum of FL after MB adsorption can be ascribed to the dye molecules electrostatically adsorbed on the FL surface. The spectroscopic results agree with the results obtained from the experiments related to the effect of ionic strength and prove that the MB adsorption by FL is based on pure electrostatic interactions and the formation of outer-sphere complexes. Spagnoli *et al.* 2017, concluded that dipole-dipole interactions between

the nitrogen in methylene blue and the phenolic groups of cashew nut shell-based carbons activated with zinc chlorid, are probably what draw methylene blue molecules to the carbon surface.
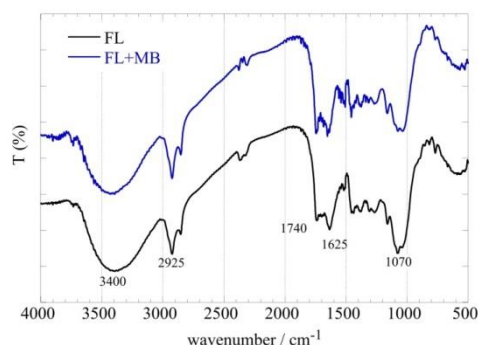

Figure 6. *FTIR* (KBr) spectra of FL prior and after adsorption of MB

3.6. Conclusions and future work

The results showed that the FL adsorbent can be satisfactorily used to remove the MB dye from aqueous solutions. *Langmuir* isotherm model best fits the adsorption data, and the kinetics of MB dye onto FL follows the pseudo-second-order model. The maximum adsorption monolayer capacity is estimated to be 95.4 mg/g at 295 K and pH 5.6. The rise in temperature from 295 K to 313 K resulted in a decrease in the adsorption capacity indicating the exothermicity of the adsorption process. In the presence of NaCl, the adsorption of MB by FL decreased, indicating the formation of outer-sphere surface complexes based on electrostatic interactions as the primary adsorption mechanism. The *FTIR* spectra (before and after adsorption) also supported this assumption, because there were no significant changes observed in the spectra upon MB dye adsorption.

To understand in depth the adsorptive behavior of FL adsorbent, future work will focus on the in-depth characterization (by XPS, SEM-EDX) and the application of FL in a) real wastewater, b) column studies, c) various types of pollutants (heavy metals, pharmaceuticals, radionuclides, pesticides, etc.). Moreover, the preparation and exploration of the applicability of biochar obtained from FL biomass for environmental application will be of particular interest.

Disclosure statement

The authors report there are no competing interests to declare.

References

Alghamdi W.M. and El Mannoubi I. (2021). Investigation of seeds and peels of Citrullus colocynthis as efficient natural adsorbent for methylene blue dye, *Processes*, **9**(8), 1279.

AL-Shehri H.S., Alanazi H.S., Shaykhayn A.M., ALharbi L.S., Alnafaei W.S., Alorabi A.Q., Alkorbi A.S. and Alharthi F.A. (2022). Adsorption of Methylene Blue by Biosorption on Alkali-Treated Solanum incanum: Isotherms, Equilibrium and Mechanism, *Sustainability*, **14**(5), 2644.

Amuda O.S., Olayiwola A.O., Alade A.O., Farombi A.G. and Adebisi S.A. (2014). Adsorption of methylene blue from aqueous solution using steam-activated carbon produced from Lantana camara stem, *Journal of Environmental Protection*, **5**(13), 1352.

Anastopoulos I. and Kyzas G.Z. (2016). Are the thermodynamic parameters correctly estimated in liquid-phase adsorption phenomena?, *Journal of Molecular Liquids*, **218**, 174–185.

Anastopoulos I. and Pashalidis I. (2019). The application of oxidized carbon derived from Luffa cylindrica for caffeine re-moval. Equilibrium, thermodynamic, kinetic and mechanistic analysis. *Journal of Molecular Liquids*, **296**, 112078.

Aragaw T.A. and Bogale F.M. (2021). Biomass-based adsorbents for removal of dyes from wastewater: a review, *Frontiers in Environmental Science*, **9**, 764958.

Basu S., Ghosh G. and Saha S. (2018). Adsorption characteristics of phosphoric acid induced activation of bio-carbon: Equilibrium, kinetics, thermodynamics and batch adsorber design, *Process Safety and Environmental Protection*, **117**, 125–142.

Besharati N., Alizadeh N. and Shariati S. (2018). Removal of cationic dye methylene blue (MB) from aqueous solution by Coffee and Peanut husk Modified with Magnetite Iron Oxide Nanoparticles, *Journal of the Mexican Chemical Society*, **62**(3), 110–124.

Blanchard G., Maunaye M. and Martin G. (1984). Removal of heavy metals from waters by means of natural zeolites. Water Research, **18**(12), 1501–1507.

Boumediene M., Benaïssa H., George B., Molina S. and Merlin A. (2018). Effects of pH and ionic strength on methylene blue removal from synthetic aqueous solutions by sorption onto orange peel and desorption study. *Journal of Materials and Environmental Sciences*, **9**(6), 1700–1711.

Bouras H.D., Isik Z., Arikan E.B., Yeddou A.R., Bouras N., Chergui A., Favier L., Amrane A. and Dizge N. (2021). Biosorption characteristics of methylene blue dye by two fungal biomasses, *International Journal of Environmental Studies*, **78**(3), 365–381.

Bulgariu L., Escudero L.B., Bello O.S., Iqbal M., Nisar J., Adegoke K.A., Alakhras F., Kornaros M. and Anastopoulos I. (2019). The utilization of leaf-based adsorbents for dyes removal: A review, *Journal of Molecular Liquids*, 276, 728–747.

Chen T., Yan B., Xu D.M. and Li L.L. (2018). Enhanced adsorption performance of methylene blue from aqueous solutions onto modified adsorbents prepared from sewage sludge, *Water Science and Technology*, **78**(4), 803–813.

Chowdhury S. and Saha P.D. 2012. Biosorption of methylene blue from aqueous solutions by a waste biomaterial: hen feathers, *Applied Water Science*, **2**(3), 209–219.

Dao M.U., Le H.S., Hoang H.Y., Tran V.A., Doan V.D., Le T.T.N. and Sirotkin A. (2021). Natural core-shell structure activated carbon beads derived from Litsea glutinosa seeds for removal of methylene blue: Facile preparation, characterization, and adsorption properties, *Environmental Research* **198**, 110481.

Deniz F. and Tezel Ersanli E. (2022). A novel biowaste-based biosorbent material for effective purification of methylene blue from water environment. *International Journal of Phytoremediation,* **24**(12), 1243–1250.

Djelloul C., Hamdaoui O. and Alghyamah A. (2021). Batch biosorption of the dye methylene blue from its aqueous solutions by Palm spathe: kinetic, isotherm, and thermodynamic studies, *Desalination and Water Treatment*, **231**, 389–397.

do Nascimento Vieira A., Kleinermanns K., Martin W.F. and Preiner M. (2020), *The ambivalent role of water at the origins of life. FEBS Letters*, **594**(17), 2717–2733.

Dos Reis G.S., Cazacliu B.G., Correa C.R., Ovsyannikova E., Kruse A., Sampaio C. H., Lima E.C. and Dotto G.L. (2020). Adsorption and recovery of phosphate from aqueous solution by the construction and demolition wastes sludge and its potential use

as phosphate-based fertiliser, *Journal of environmental chemical engineering*, **8**(1), 103605.

Dotto G.L., Pinto L.A.A., Hachicha M.A. and Knani S. (2015). New physicochemical interpretations for the adsorption of food dyes on chitosan films using statistical physics treatment, *Food chemistry*, **171**, 1–7.

Dutta S., Gupta B., Srivastava S.K. and Gupta A.K. (2021). Recent advances on the removal of dyes from wastewater using various adsorbents: A critical review, *Materials Advances*, **2**(14), 4497–4531.

Fakioğlu M. and Kalpaklı Y. (2022). Mechanism and behavior of caffeine sorption: affecting factors. *RSC Advances,* **12**(41), 26504–26513.

Fan S., Tang J., Wang Y., Li H., Zhang H., Tang J., Wang Z. and Li X. (2016). Biochar prepared from co-pyrolysis of municipal sewage sludge and tea waste for the adsorption of methylene blue from aqueous solutions: Kinetics, isotherm, thermodynamic and mechanism. *Journal of Molecular Liquids*, **220**, 432–441.

Fernandez R.D., Ceballos S.J., Aragón R., Malizia A., Montti L., Whitworth-Hulse J.I., Castro-Díez P. and Grau H.R. (2020). A global review of *Ligustrum lucidum* (*OLEACEAE*) invasion. *The Botanical Review*, **86,** 93–118.

Freundlich H.M.F. (1906). Over the adsorption in solution. The *Journal of Physical Chemistry*, **57**(385471), 1100–1107.

Gao Y., Zeng J., Zhu S. and Liu Q. (2021). Co-modification of lignocellulosic biomass by maleic anhydride and ferric hydroxide for the highly efficient biosorption of methylene blue. *New Journal of Chemistr*y, **45**(42), 19678–19690.

Geng Y., Zhang J., Zhou J. and Lei J. (2018). Study on adsorption of methylene blue by a novel composite material of TiO2 and alum sludge. *RSC Advances*, **8**(57), 32799–32807.

Han R., Zou W., Yu W., Cheng S., Wang Y. and Shi J. (2007). Biosorption of methylene blue from aqueous solution by fallen phoenix tree's leaves. *Journal of Hazardous Materials*, **141**(1), 156–162.

Hevira L., Ighalo J.O., Aziz H. and Zein R. (2021). *Terminalia catappa* shell as low-cost biosorbent for the removal of methylene blue from aqueous solutions. *Journal of industrial and engineering chemistry*, **97**, 188–199.

Hosny N.M. and Gomaa Elmahgary M.G. (2023). Adsorption of polluted dyes from water by transition metal oxides: A review. *Applied Surface Science Advances*, **15**, 100395.

Hossen A., Chowdhury T. and Mondal I.H. (2022). Purification of textile dye-contained wastewater by three alternative promising techniques: Adsorption, Biodegradation and Advanced Oxidation Processes (AOPs) - A review. *Textile Engineering & Fashion Technology*, **8**(3), 96–98.

Ighalo J.O., Iwuozor K.O., Igwegbe C.A. and Adeniyi A.G. (2021). Verification of pore size effect on aqueous-phase adsorption kinetics: a case study of methylene blue. Colloids and Surfaces A: *Physicochemical and Engineering Aspects*, **626**, 127119.

Kandisa R.V., Saibaba K.N., Shaik K.B. and Gopinath R. (2016). Dye removal by adsorption: a review. *Journal of Bioremediation & Biodegradation*, **7**, 371(6).

Kandisa R.V., Kv N.S., Gopinadh R. and Veerabhadram K. (2018). Kinetic Studies on Adsorption of Methylene Blue Using Natural Low Cost Adsorbent. *Journal of Industrial Pollution Control Journal of Industrial Pollution Control*, **34**, 2054–2058.

Kini M.S., Saidutta M.B. and Murty V.R. (2014). Studies on biosorption of methylene blue from aqueous solutions by powdered palm tree flower (*Borassus flabellifer*). *International Journal of Chemical Engineering*, 2014, 306519.

Lagergren S. (1898). About the Theory of So-Called Adsorption of Soluble Substances. *Kungliga Svenska Vetenskapsakademiens Handlingar*. **24**, 1–39.

Langmuir I. (1918). The adsorption of gases on plane surfaces of glass, mica and platinum. *Journal of the American Chemical Society*, **40**(9), 1361–1403.

Li Y., Li H., Jiang S., Zhou Y., Cao D., Che X., Yang Y., Shang J. and Cheng X. (2022). Enhanced adsorption for fluoroquinolones by MnOx-modified palygorskite composites: preparation, properties and mechanism. *Separation and Purification Technology*, **299**, 121468.

Lima E.C., Hosseini-Bandegharaei A., Moreno-Piraján J.C. and Anastopoulos I. (2019). A critical review of the estimation of the thermodynamic parameters on adsorption equilibria. Wrong use of equilibrium constant in the Van't Hoof equation for calculation of thermodynamic parameters of adsorption. *Journal of Molecular Liquids*, **273**, 425–434.

Nath H., Saikia A., Goutam P.J., Saikia B.K. and Saikia N. (2021). Removal of methylene blue from water using okra (*Abelmoschus esculentus* L.) mucilage modified biochar. *Bioresource Technology Reports*, **14**, 100689.

Ncibi M.C., Mahjoub B. and Seffen M. (2007). Kinetic and equilibrium studies of methylene blue biosorption by *Posidonia oceanica* (L.) fibres. *Journal of Hazardous Materials*, **139**(2), 280–285.

Nipa S.T, Shefa N.R., Parvin S., Khatun M.A., Alam M.J., Chowdhury S., Khan M.A.R., Zaker Shawon Sk.Md.A., Biswas B.K. and Rahman M.W. (2023). Adsorption of methylene blue on papaya bark fiber: Equilibrium, isotherm and kinetic perspectives. *Results in Engineering*, **17**, 100857.

Pang X., Sellaoui L., Franco D., Netto M.S., Georgin J., Dotto G.L., Abu Shayeb M.K., Belmabrouk H., Bonilla-Petriciolet A. and Li, Z. (2020). Preparation and characterization of a novel mountain soursop seeds powder adsorbent and its application for the removal of crystal violet and methylene blue from aqueous solutions. *Chemical Engineering Journal*, **391**, 123617.

Pathania D., Sharma S. and Singh P. (2017). Removal of methylene blue by adsorption onto activated carbon developed from *Ficus carica* bast. *Arabian Journal of Chemistry*, **10**, S1445-S1451.

Pavan F.A., Lima E.C., Dias S.L. and Mazzocato A.C. (2008). Methylene blue biosorption from aqueous solutions by yellow passion fruit waste. *Journal of Hazardous Materials*, **150**(3), 703–712.

Rangabhashiyam S., Lata S. and Balasubramanian P. (2018). Biosorption characteristics of methylene blue and malachite green from simulated wastewater onto *Carica papaya* wood biosorbent. *Surfaces and Interfaces*, **10**, 197–215.

Rani S. and Mahajan R.K. (2016). Equilibrium, kinetics and thermodynamic parameters for adsorptive removal of dye Basic Blue 9 by ground nut shells and Eichhornia. *Arabian Journal of Chemistry*, **9**, S1464-S1477.

Santos R.K., Nascimento B.F., de Araújo C.M., Cavalcanti J.V., Bruckmann F.S., Rhoden C.R., Dotto G.L., Oliveira M.L.S., Silva L.F.O. and Sobrinho M.A.M. (2023). Removal of chloroquine from the aqueous solution by adsorption onto açaí-based biochars: Kinetics, thermodynamics, and phytotoxicity. *Journal of Molecular Liquids*, **383**, 122162.

Sharma Y.C. and Uma. (2010). Optimization of parameters for adsorption of methylene blue on a low-cost activated carbon. *Journal of Chemical & Engineering Data*, **55**(1), 435–439.

Silva F., Nascimento L, Brito M., da Silva K., Paschoal Jr W. and Fujiyama R. (2019). Biosorption of methylene blue dye using natural biosorbents made from weeds. *Materials*. **12**(15), 2486.

Spagnoli A.A., Giannakoudakis D.A. and Bashkova S. (2017). Adsorption of methylene blue on cashew nut shell based carbons activated with zinc chloride: The role of surface and structural parameters. *Journal of Molecular Liquids*, **229**, 465–471.

Taweekarn T., Wongniramaikul W., Boonkanon C., Phanrit C., Sriprom W., Limsakul W., Towanlong W., Phawachalotorn C. and Choodum A. (2022). Starch Biocryogel for Removal of Methylene Blue by Batch Adsorption. *Polymer*s, **14**(24): 5543.

Thabede P., Shooto N. and Naidoo E. (2021). Sorption of chromium (VI), cadmium (II) ions and methylene blue dye by pristine, defatted and carbonized *Nigella sativa* L. seeds from aqueous solution. *Asian Journal of Chemistry*, **33**(2): 471–483.

Wang X., Jiang J. and Gao W. (2022). Reviewing textile wastewater produced by industries: Characteristics, environmental impacts, and treatment strategies. *Water Science and Technology*, **85**(7), 2076–2096.

Zein R., Purnomo J.S., Ramadhani P., Alif M.F. and Putri C.N. (2023). Enhancing sorption capacity of methylene blue dye using solid waste of lemongrass biosorbent by modification method. *Arabian Journal of Chemistry*, **16** (2), 104480.

Zhou Y., Lu J., Zhou Y. and Liu Y. (2019). Recent advances for dyes removal using novel adsorbents: A review. *Environmental pollution*, **252**, 352–365.